

TTK predicts triple positive breast cancer prognosis and regulates tumor proliferation and invasion

Yun-He GAO, Shan-Shan QU, Lan-Qing CAO, Min YAO*

Department of Pathology, The Second Hospital of Jilin University, Changchun, Jilin, China

*Correspondence: yaomin@jlu.edu.cn

Received April 21, 2021 / Accepted August 3, 2021

This study was conducted to investigate the expression of the spindle assembly checkpoint kinase tyrosine/threonine kinase (TTK) in triple positive breast cancer (TPBC) and its effect on TPBC cells. We analyzed the status of TTK in 69 TPBC samples using immunohistochemistry. The correlation between TTK and clinicopathological parameters was analyzed using a chi-squared test. The prognostic value of TTK was evaluated using Kaplan-Meier survival curves. We analyzed the role of TTK in the invasion and proliferation of TPBC cells *in vitro* and *in vivo*. The mean age of the 69 patients with TPBC enrolled in this study was 53 years (range: 29-86 years). TTK expression was positively correlated with tumor size ($p=0.034$), p53 status ($p=0.023$), TNM stage ($p=0.023$), and Ki-67 index ($p<0.001$). The Kaplan-Meier curves revealed that TTK expression was correlated with poor disease-free survival ($p=0.001$) and overall survival ($p=0.050$). Multivariate proportional hazard regression analyses showed that TTK and TNM staging were significant independent predictors of disease-free survival ($p=0.007$ and $p=0.034$, respectively). Additionally, TTK knockdown inhibited the invasion and proliferation of the BT474 TPBC cell line. The findings of this study indicate that TTK overexpression is associated with cancer progression and prognosis in patients with TPBC, whereas TTK knockdown inhibits the invasion and proliferation of TPBC cells. Thus, TTK might serve as a prognostic marker for TPBC.

Key words: overall survival, disease-free survival, prognosis, cancer, spindle assembly checkpoint

Understanding breast cancer biology is important in terms of both therapy management and the assessment of patient outcomes. Breast cancer has been classified into different subtypes based on the expression of estrogen receptors (ERs), progesterone receptors, and human epidermal growth factor receptor 2 (HER2). Recently, a distinct subcategory of HER2-enriched breast cancer with positive hormone receptors has been identified (HER2-positive breast cancer). This subtype exhibits high levels of hormone receptor expression and is referred to as “triple positive” breast cancer (TPBC). In ER+ luminal tumors, preclinical evidence suggests that strong crosstalk occurs between the ER and HER2 signaling pathways and that the activation of the ER pathway leads to resistance to the anti-HER2 therapy; furthermore, from a genomic/transcriptomic perspective, ER+/HER2+ tumors might be much more common than ER-/HER2+ tumors and have fewer tumor-infiltrating lymphocytes and lower PD-L1 expression [1, 2]. Current treatment guidelines, however, do not propose distinct management strategies for ER+/HER2+ and ER-/HER2+ breast cancer [3, 4]. TPBC responds distinctly to conventional treatment [5]. This raises

the question of whether it is necessary to tailor TPBC therapy to individuals.

The spindle assembly checkpoint is a signaling cascade that prevents chromosome mis-segregation by arresting mitosis until all chromosomes are properly attached to the mitotic spindle [6]. As the core spindle assembly checkpoint kinase, tyrosine/threonine kinase (TTK) is a dual-specificity kinase that can phosphorylate serine/threonine and tyrosine residues [7]. TTK is critical for the recruitment of spindle assembly checkpoint proteins to unattached kinetochores, mitotic checkpoint complex formation, and mitotic arrest [8]. The inhibition of TTK activity causes cells to prematurely exit mitosis with unattached chromosomes, resulting in severe chromosome mis-segregation, aneuploidy, and eventually cell death [9–12]. The overexpression of mitotic checkpoint genes leads to chromosomal instability in cancer cells [13–16].

Previous studies have shown that TTK is overexpressed in breast cancer cells, particularly in the HER2+ and triple negative breast cancer (TNBC) subtypes [13, 14, 17, 18]. However, whether TTK is also a prognostic factor in TPBC

remains unclear. In this study, we analyzed the expression of TTK in TPBC and further analyzed its biological function during disease progression.

Patients and methods

TPBC tissue and cell line. We retrospectively collected data and tissue specimens from 69 patients with TPBC who had undergone tumor surgical resection at the Second Hospital of Jilin University between January 2009 and January 2013. The patients had been diagnosed with invasive carcinoma of no special type. The last follow-up was conducted in April 2018 (mean follow-up duration: 44.2 months, range: 1.67–72.10 months). Patients administered preoperative neoadjuvant chemotherapy or hormonal treatment were excluded from this study.

Clinicopathological data were retrieved from patient medical records. These parameters included patient age at initial diagnosis, histological subtype, tumor size, lymph node metastasis, and clinical outcome. The study protocol was approved by the Institutional Ethics Committee of the Second Hospital of Jilin University, Jilin, China (IRB approval number: 2020008). The need for written informed consent was waived because of the retrospective nature of the study.

Two-micrometer-thick sections were prepared from paraffin blocks of breast cancer tissues retrieved from the Pathology Department, Second Hospital of Jilin University, for immunohistochemistry and hematoxylin and eosin staining. The latter was used to confirm the diagnoses, and the results were reviewed by Min Yao and Yunhe Gao. Tumor histological grades were assessed using the Nottingham grading system [19]. A human breast carcinoma cell line, BT474, which is a TPBC cell line, was purchased from the American Type Culture Collection (Manassas, VA, USA). The cell line was maintained in RPMI-1640 supplemented with 10% fetal bovine serum at 37°C in a humidified atmosphere with 5% CO₂.

Immunohistochemistry. Immunohistochemical staining was performed automatically using the PT Link Pre-Treatment system and Autostainer Link 48 system (both from DAKO, Carpinteria, CA, USA). Endogenous peroxidases were quenched with 3% H₂O₂ for 10 min. The sections were incubated with primary antibodies against TTK (Cat. #AF6028; NOVUS, St. Louis, MI, USA; 1:200 dilution in phosphate-buffered saline [PBS]), as well as AKT (Cat. #4691) and Ki-67 (Cat. #9449) from Cell Signaling Technology (Danvers, MA, USA) at 1:300 dilution in PBS, for 30 min, followed by application of the secondary biotinylated antibody for 20 min. The slides were stained using 3, 3'-diaminobenzidine and counterstained with hematoxylin.

Review and scoring of immunostained tissue sections. The immunostained tissue sections were independently reviewed and scored by two investigators to determine the immunostaining percentage and staining intensity, as

described previously [20]. A numerical final expression score (FS) was calculated for each tissue sample by multiplying the staining intensity (I) score (0, negative; 1, weak; 2, moderate; 3, strong staining) by the percentage (P) of positively stained cells (FS=P×I). The final expression score, therefore, ranged from 0 to 300. Thereafter, each case was scored as positive or negative using the median final expression score as the cutoff value for statistical analysis [21].

Cell proliferation and colony formation experiments. Cells were seeded into 96-well plates at a density of 5.0×10³ cells/well and cultured for 24 h. The cells were then incubated with 10 μl of CCK-8 (Beyotime Biotechnology LLC, Shanghai, China) solution for 30–45 min at 37°C. Absorbance at 450 nm was detected with a microplate reader (Model 680; Bio-Rad, Hercules, CA, USA). The cell inhibitory index was calculated as $[1 - (A_{450_{\text{sample}}} - A_{450_{\text{blank}}}) / (A_{450_{\text{control}}} - A_{450_{\text{blank}}})] \times 100\%$. The transfected cells were seeded into a culture plate at 200 cells/well, and after 2 weeks of incubation, the cells were washed with PBS and stained with Giemsa solution. The number of colonies containing >50 cells was counted under a microscope.

Western blot analysis. Cells were lysed using RIPA buffer (Beyotime Biotechnology), vortexed for 30 s, and centrifuged at 14,000×g for 5 min. The supernatants were collected and stored at -20°C. The whole-cell lysates were resolved by SDS-PAGE, and the proteins were blotted onto a nitrocellulose membrane. The expression of various proteins was detected using primary antibodies against the following: TTK (Cat. #AF6028; NOVUS; 1:500 dilution in PBS); AKT (Cat. #4691), CCND1 (Cat. #55506), CCND2 (Cat. #3741), CDK4 (Cat. #12790), CDK6 (Cat. #13331), p21 (Cat. #2947), E-cadherin (Cat. #14472), N-cadherin (Cat. #13116), vimentin (Cat. #5741), and Snail (Cat. #3879) from Cell Signaling Technology at 1:1000 dilution in PBS, and β-actin (Cat. #HC201-01; TransGen Biotechnology LLC, Beijing, China; 1:1000 dilution in PBS). The corresponding secondary antibodies were anti-mouse and anti-rabbit antibodies. Immunoreactive bands were visualized via enhanced chemiluminescence.

The 5-ethynyl-2'-deoxyuridine (EdU) proliferation assay. To demonstrate the effect of TTK on the proliferation of BT474 cells, an EdU proliferation assay was performed according to the manufacturer's instructions. The cells were incubated with 50 μM EdU for 2 h and stained with ADO-Lo and 4',6-diamidino-2-phenylindole (DAPI). The number of EdU-positive cells was detected via fluorescence microscopy. The display rate of EdU-positive cells was calculated as the ratio of the number of EdU-positive cells to the total number of DAPI-stained cells (blue cells).

Cell transfection. A TTK-targeting short hairpin RNA (shRNA) plasmid, pLVshRNA-EGFP(2A)Puro-TTK-shRNA1 (#P11886; MiaoLingBio, Changchun, China), which also expressed green fluorescent protein, was constructed and transfected into BT474 cells. A functional, nontargeting shRNA, and an empty vector were used as controls.

Quantitative reverse transcription-PCR (qRT-PCR).

Total RNA was isolated from 5×10^6 cells using TRIzol reagent (Invitrogen, Carlsbad, CA, USA) according to the manufacturer's instructions. Total RNA concentration and purity were analyzed in duplicate samples using a NanoDropND-2000 spectrophotometer (Thermo Fisher Scientific, Waltham, MA, USA). cDNA was synthesized from qualified RNA using an RT-PCR reverse transcription kit (TransGen Biotechnology LLC), and 1 μ g of total RNA was reverse-transcribed into cDNA under the following conditions: 25°C for 10 min, 42°C for 30 min, and 85°C for 5 s, as per the manufacturer's recommendations. The cDNA was stored at -20°C until use. PCR was performed using a PCR kit (TransGen Biotechnology LLC), and the PCR products were electrophoresed on 1.5% agarose gels. qRT-PCR was conducted with either Taq-Man or SYBR Green PCR reagents on an ABI Prism 7300 detection system (all from Applied Biosystems, Foster City, CA, USA). The reaction program was as follows: 95°C for 3 min, followed by 40 cycles at 95°C for 30 s and 55°C for 20 s, and finally, 72°C for 15 s. *GAPDH* served as an internal control, and relative mRNA levels were calculated using the $2^{-\Delta\Delta Ct}$ method [22]. The following primers were synthesized by Sangon Biotech (Shanghai, China): TTK, (qRT-PCR)-forward: TCCCCAGCGCAGCTTTCTGTAGA; TTK, (qRT-PCR)-reverse: CCAGTCCTCTGGGTTGTTTGCCAT; *GAPDH*, (qRT-PCR)-forward: GGAGC-GAGATCCCTCCAAAAT; *GAPDH*, (qRT-PCR)-reverse: GGCTGTTGTCATACTTCTCATGG.

Transwell invasion assay. The transfected cells were inoculated into the upper chamber of a Transwell chamber (Corning, Inc., Corning, NY, USA) at 1×10^5 cells/ml, and RPMI-1640 medium supplemented with 30% fetal bovine serum was added to the lower chamber. The cells were cultured in 5% CO₂ and 100% humidity and at a 37°C constant temperature for 24 h. The chamber was removed, and the cells were rinsed with PBS and fixed in absolute ethanol for 40 min. After crystal violet staining, the cells that did not pass through the upper chamber were wiped off using a cotton swab, and cells that had passed through the upper chamber were counted under an inverted microscope. Finally, invasive cells on the lower surface of the membrane were counted using a microscope. Five fields of view were randomly selected to detect changes in invasion ability. The experiment was repeated three times.

Animal studies. Fourteen female BALB/c nude mice (6-weeks-old) were purchased from SPF Biotechnology (Beijing, China) and randomized into two groups. All animal experiments were conducted in accordance with the institutional guidelines and approved by the Experimental Animal Ethical Committee of Jilin University. Cells were injected subcutaneously into the right buttock of each mouse at 1×10^6 cells per 0.1 ml PBS. All mice were maintained in a standardized barrier system environment at the Animal Experiment Center of the Basic Medical College of Jilin. After 4 weeks of observation, the mice were euthanized. The xenograft tumors

were removed and fixed in 10% formalin. The tumors were measured using Vernier calipers, and the volume was calculated using the following formula: $V = (\text{width}^2 \times \text{length}) / 2$ [23]. The xenograft tumors were examined macroscopically and subjected to hematoxylin and eosin staining and immunohistochemistry.

Statistical analyses. All statistical analyses were performed using SPSS v. 21.0 (SPSS, Inc, Chicago, IL, USA). Continuous variables were evaluated using the Mann-Whitney U test, whereas categorical variables were analyzed with the chi-squared test. Furthermore, significant variables ($p < 0.05$) from the univariate analyses were included in multivariate analyses. A multivariate Cox proportional hazards model was used to obtain hazard ratios for survival and to identify factors affecting disease-free survival (DFS) and overall survival (OS). Kaplan-Meier survival curves and log-rank tests were used to evaluate DFS and OS. Experiments were repeated at least three times. A p -value < 0.05 was considered to indicate statistically significant differences.

Results

Patient characteristics. The median age of the 69 patients with invasive breast cancer included in this study was 53 years (range: 29–86 years). According to the seventh edition of the UICC cancer staging system grouping criteria, 17.4% (12/69), 43.5% (30/69), and 39.1% (27/69) of the TPBC patients had stage I, II, and III disease, respectively. All patients exhibited invasive breast ductal carcinoma and underwent a modified radical mastectomy. Among the patients with available adjuvant treatment information, 97.1% (67/69) were administered chemotherapy (two ceased treatment because of an allergic reaction) and 33.3% (23/69) were treated with radiation.

Associations between TTK expression and clinicopathological parameters in patients with breast cancer. The associations between TTK expression and clinicopathological parameters were analyzed using Pearson's χ^2 test (Table 1). TTK positivity was observed in 39.1% (27/69) of TPBC tissues (Figure 1A). TTK expression was positively associated with tumor size ($p = 0.034$), p53 mutation ($p = 0.023$), TNM stage ($p = 0.023$), and Ki-67 expression ($p < 0.001$). The larger tumor size and higher Ki-67 expression with TTK overexpression suggest that TPBC is more proliferative and has higher cell survival than TTK-negative TPBC. Furthermore, the p53 mutation and advanced TNM stages associated with TTK overexpression indicate that TPBC has more aggressive clinicopathological features than other forms of breast cancer.

Association between TTK expression and patient survival. Kaplan-Meier curves and a log-rank test were used to analyze OS and DFS after stratification by TTK expression. TTK expression was significantly correlated with DFS ($p = 0.001$, Figure 1B) and OS ($p = 0.050$, Figure 1B). We further investigated the prognostic value of various clini-

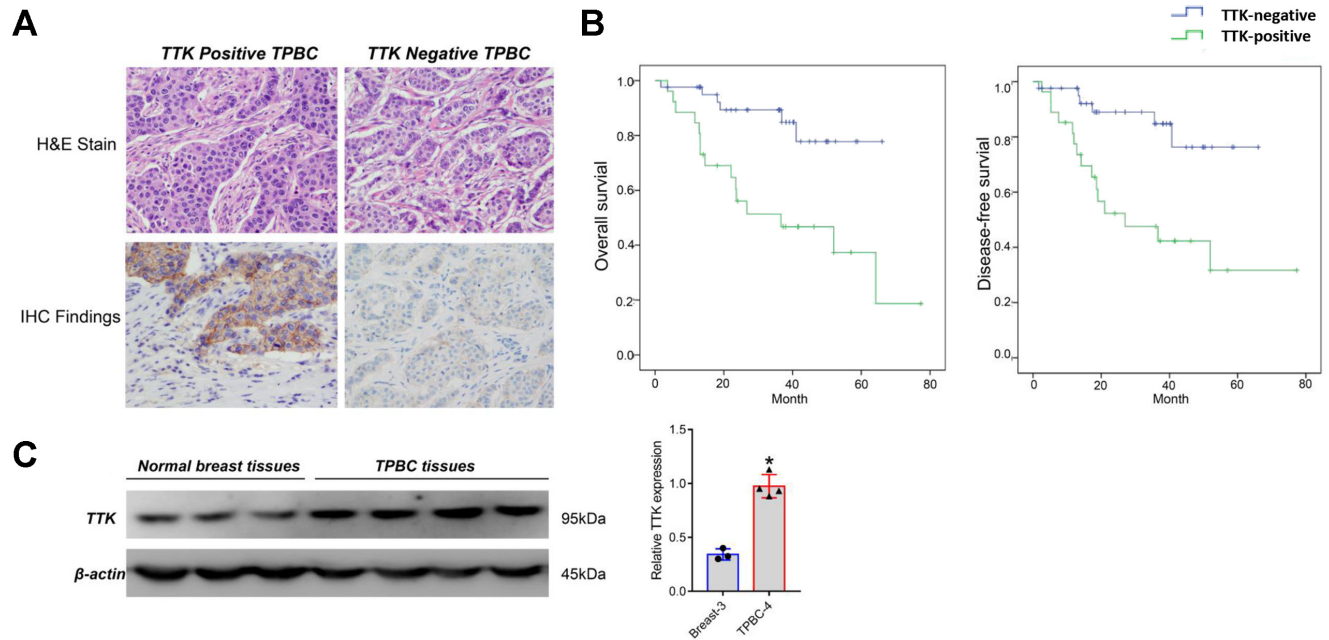


Figure 1. TTK expression in triple positive breast cancer (TPBC) tissues. A) Positive and negative expression of TTK in breast cancer tissues (original magnification $\times 100$). B) Higher TTK expression could predict shorter disease-free survival and overall survival for TPBC patients ($p=0.001$ and $p=0.050$). C) TTK protein expression in normal breast tissues and TPBC tissues was detected via western blotting.

Table 1. Association between TTK expression and clinicopathological parameters of patients with triple positive breast cancer.

Characteristics	No.	TTK expression		p-value
		Negative No. (%)	Positive No. (%)	
Age (years)	<50	18	6	0.558
	≥ 50	51	21	
Size (cm)	≤ 2	30	9	0.034
	2–5	30	11	
	>5	9	7	
Histology grade	1	3	0	0.121
	2	63	27	
	3	3	0	
Lymph node status	Negative	24	10	0.715
	1–3	18	8	
	4–9	12	6	
	>9	15	9	
TNM stage	I	12	3	0.023
	II	30	8	
P53 status	III	27	16	0.023
	wild-type	49	15	
BCL-2 status	mutant-type	20	12	0.270
	Negative	12	3	
Ki-67 status	Positive	57	24	<0.001
	$\leq 20\%$	30	3	
	>20%	39	24	

Abbreviations: TNM-Tumor Node Metastasis; TTK-tyrosine/threonine kinase

copathological parameters using Kaplan-Meier curves and a log-rank test (Table 2). This revealed a significant association between DFS and tumor size ($p=0.020$), p53 mutation ($p=0.005$), TTK status ($p=0.001$), and TNM stage ($p<0.001$). OS was significantly associated with tumor size ($p=0.044$), BCL-2 status ($p=0.001$), p53 mutation ($p<0.001$), Ki-67 index ($p=0.014$), TTK status ($p=0.050$), and TNM stage ($p=0.038$). Significant parameters were selected for multivariate analysis

Table 2. Univariate analyses of disease-free survival and overall survival for patients with triple positive breast cancer.

	DFS		OS	
	Log rank	p-value	Log rank	p-value
Histology grade (II/ III vs. I)	1.667	0.435	1.955	0.376
Age (<50 vs. ≥ 50)	0.019	0.890	0.042	0.838
Tumor size (2–5 cm/ >5 cm vs. 2 cm)	7.817	0.020	6.228	0.044
Lymph node status (Present vs. Absent)	4.883	0.181	4.419	0.220
BCL-2 (Positive vs. Negative)	2.004	0.157	10.667	0.001
P53 (Mutant vs. Wild)	7.96	0.005	13.636	<0.001
Ki-67 (>20% vs. $\leq 20\%$)	2.009	0.147	6.000	0.014
TTK (Positive vs. Negative)	10.490	0.001	5.997	0.050
TNM (II/ III vs. I)	25.737	<0.001	4.316	0.038

Abbreviations: TNM-Tumor Node Metastasis; TTK-tyrosine/threonine kinase

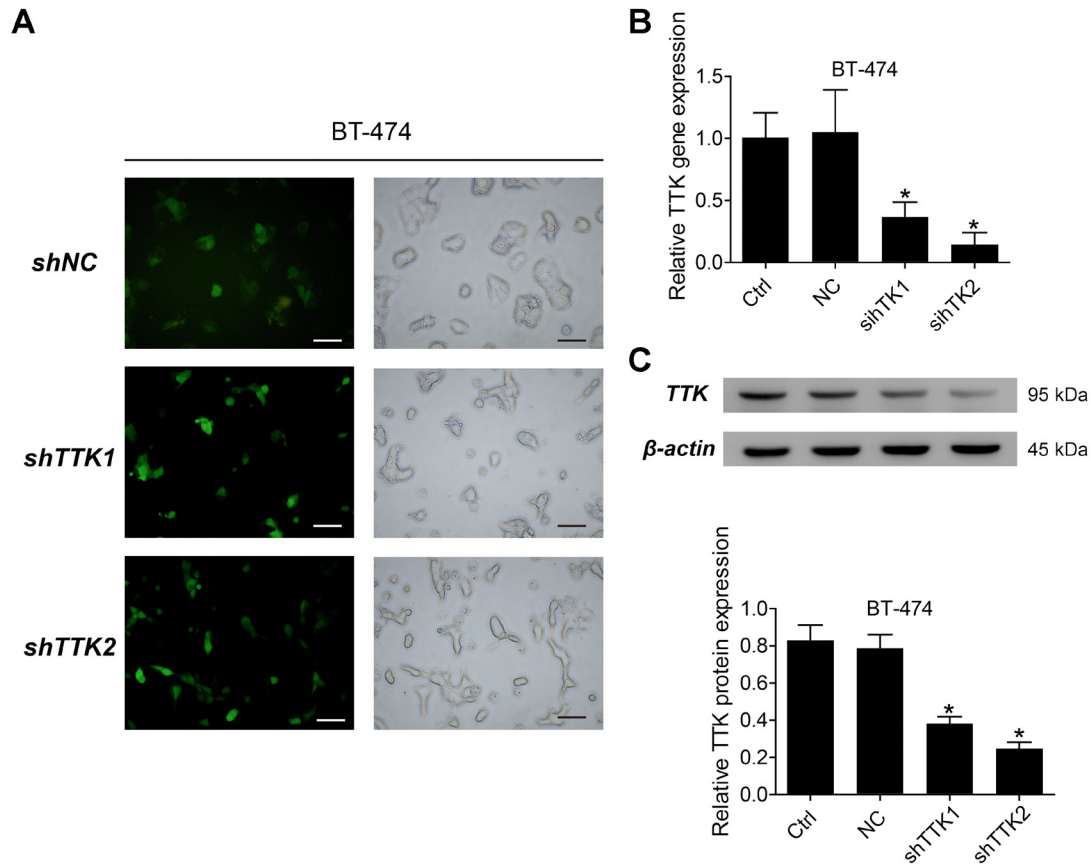


Figure 2. Effects of *TTK* knockdown in BT474-TS cells. A) Green fluorescent protein expression in BT474-TS cells, detected by confocal microscopy. B) mRNA levels of *TTK* in BT474-TS cells detected by RT-PCR. C) *TTK* protein expression in BT474-TS cells, detected by western blotting. Data are presented as the mean \pm SD. The data shown are representative results of three independent experiments. * $p < 0.05$

Table 3. Multivariate analyses of disease-free survival and overall survival for patients with triple positive breast cancer.

	DFS			OS		
	HR	95% CI	p-value	HR	95% CI	p-value
Histology grade (II/ III vs. I)	NA	NA	NA	NA	NA	NA
Age (<50 vs. \geq 50)	NA	NA	NA	NA	NA	NA
Tumor size (2–5 cm/ >5 cm vs. 2 cm)	0.598	0.499–3.399	0.598	1.519	0.572–4.034	0.401
Lymph node status (Present vs. Absent)	1.012	0.641–1.598	0.96	2.509	0.304–1.44	0.298
BCL-2 (Positive vs. Negative)	NA	NA	NA	0.984	0.195–4.957	0.984
P53 (mutant vs. wild)	2.27	0.911–5.661	0.079	45.164	0.144–141.490	0.194
Ki-67 (>20% vs. \leq 20%)	0.928	0.517–1.664	0.801	1.341	0.315–1.570	0.745
<i>TTK</i> (Positive vs. Negative)	3.736	1.439–9.696	0.007	0.984	0.195–4.957	0.985
TNM (II/ III vs. I)	2.337	1.042–4.769	0.034	2.179	0.436–11.076	0.322

Abbreviations: CI-Confidence Interval; HR-Hazard Ratio; TNM-Tumor Node Metastasis; *TTK*-tyrosine/threonine kinase

(Table 3). In the multivariate Cox regression model, *TTK* and TNM staging were identified as significant independent predictors of DFS ($p=0.007$ and $p=0.034$, respectively) among all patients with TPBC (Table 3). *TTK* expression was also significantly higher in TPBC tissues than in normal breast tissues, according to western blot analysis (Figure 1C).

TTK knockdown inhibits TPBC cell proliferation. To investigate the potential role of *TTK* in TPBC cells, we designed and tested *TTK*-targeting shRNAs and identified two that effectively knocked down *TTK* expression in BT474 cells (Figures 2A, 2B). The CCK-8 assay showed that the survival rate of BT474 cells was significantly reduced after

TTK knockdown (shTTK group vs. control group, $p < 0.001$; Figure 3A). Furthermore, colony formation ability experiments and an EdU assay were performed to mimic the ability of cells to form multicellular clones from individual tumor cells (Figures 3B, 3C). The number of BT474 cells in the shTTK group was remarkably lower than that in the control group ($p < 0.05$ and $p < 0.05$). Furthermore, in the shTTK group, *CCND1*, *CCND2*, *CDK4*, *CDK6*, and *p21* expression levels were significantly lower than those in the control group (Figure 3D). These findings suggest that downregulation of *TTK* can significantly inhibit the proliferation of the BT474 TPBC cell line and reduce colony formation. After transfection with *TTK*-targeting shRNA, AKT expression was significantly lower in BT474 cells than in control cells (Figure 3D).

TTK knockdown inhibits the invasiveness of TPBC cells. Epithelial-mesenchymal transition (EMT), an invasive phenotype of cancer cells, plays a key role in tumor metastasis. Western blot analysis revealed that the expression of EMT proteins (E-cadherin, vimentin, N-cadherin, and Snail) was significantly altered by *TTK* knockdown. The expression of E-cadherin was significantly higher, and that of vimentin, N-cadherin, and Snail protein was significantly lower, in the shTTK group than in the control group (Figure 4A). The Transwell assay results revealed the effects of *TTK* knockdown on the invasiveness of BT474 cells. There were significantly fewer invading cells in the shTTK group than

in the control group ($p = 0.005$; Figure 4B). These results suggest that *TTK* enhances the invasiveness of BT474 cells by regulating EMT.

TTK knockdown inhibits tumor growth in a breast cancer xenograft model. *TTK* suppression was examined in nude mice bearing established control and shTTK BT474 xenograft tumors. *TTK* suppression inhibited tumor growth in the shTTK group compared to that in the control group in this xenograft model (Figure 5A). Moreover, based on the tumor tissue immunohistochemistry results, *TTK*, AKT, and Ki-67 expressions were suppressed in the shTTK group relative to that in the control group (Figures 5B, 5C); this is consistent with the *in vitro* results. These results indicate that *TTK* enhances tumor growth *in vivo*, possibly via the AKT pathway.

Discussion

In this study, we found that *TTK* expression enhanced the proliferation and metastasis of BT474 TPBC cells. Furthermore, unlike that in TNBC, *TTK* overexpression was associated with a worse prognosis in patients with TPBC. Encouraging results have been obtained using a dual blockade strategy comprising anti-HER2 agents and hormonal therapy [24]. Patients with the HER2-enriched molecular subtype of breast cancer and those at high risk of relapse are typically

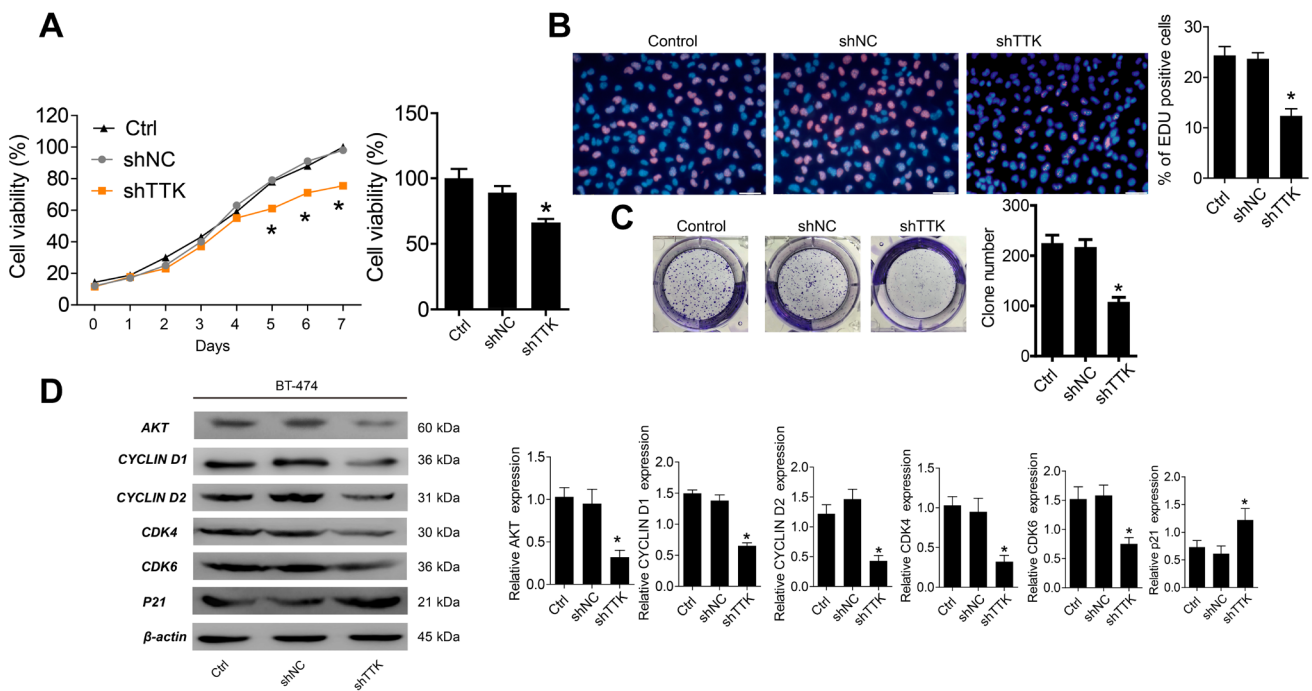


Figure 3. *TTK* knockdown inhibits the proliferation of triple positive breast cancer (TPBC) cells. **A**) CCK-8 assay to detect the effects of *TTK* knockdown on BT474-TS cell proliferation. **B**) EdU assay to detect the proliferation of *TTK*-knockdown and control group cells (magnification $\times 40$). **C**) Colony formation assays were performed to detect the number of clones formed by *TTK*-knockdown and control group cells (magnification $\times 20$). **D**) Western blot analysis of proliferation-related protein expression. Data are presented as the mean \pm SD. The data shown are representative results of three independent experiments. * $p < 0.05$

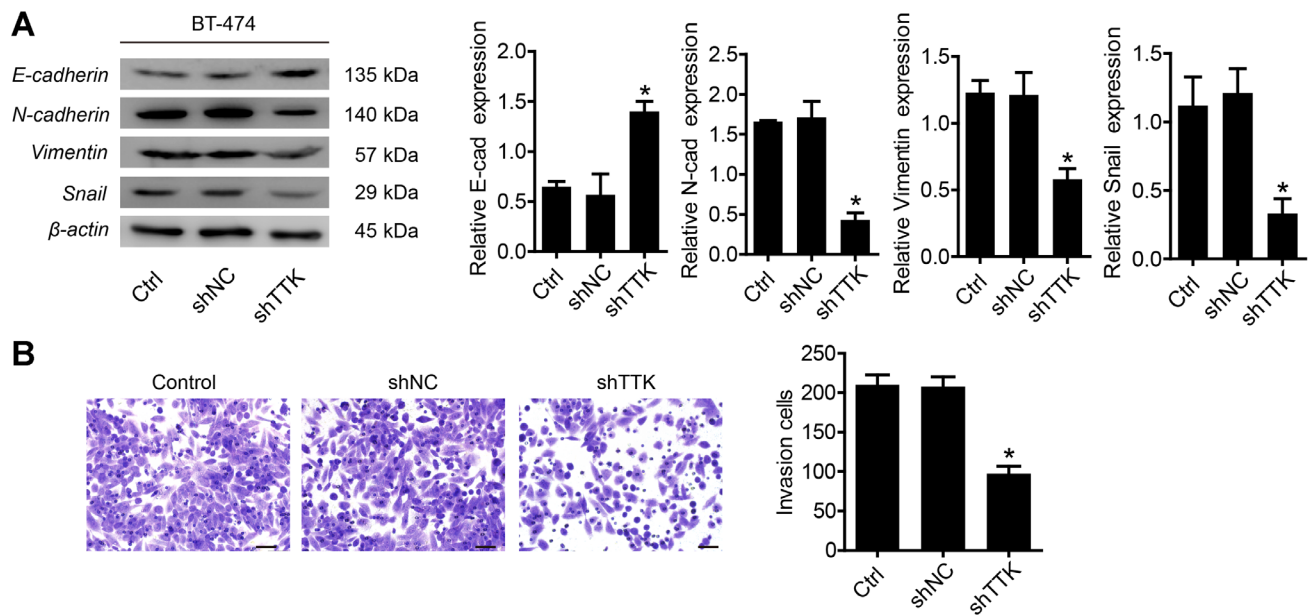


Figure 4. *TTK* knockdown inhibits invasion of triple positive breast cancer (TPBC) cells. **A**) Western blot analysis of epithelial-mesenchymal transition (EMT)-related protein expression. **B**) Transwell assay to assess migration and invasion of TPBC cells. Data are presented as the mean \pm SD. The data shown are representative results of three independent experiments. * $p < 0.05$

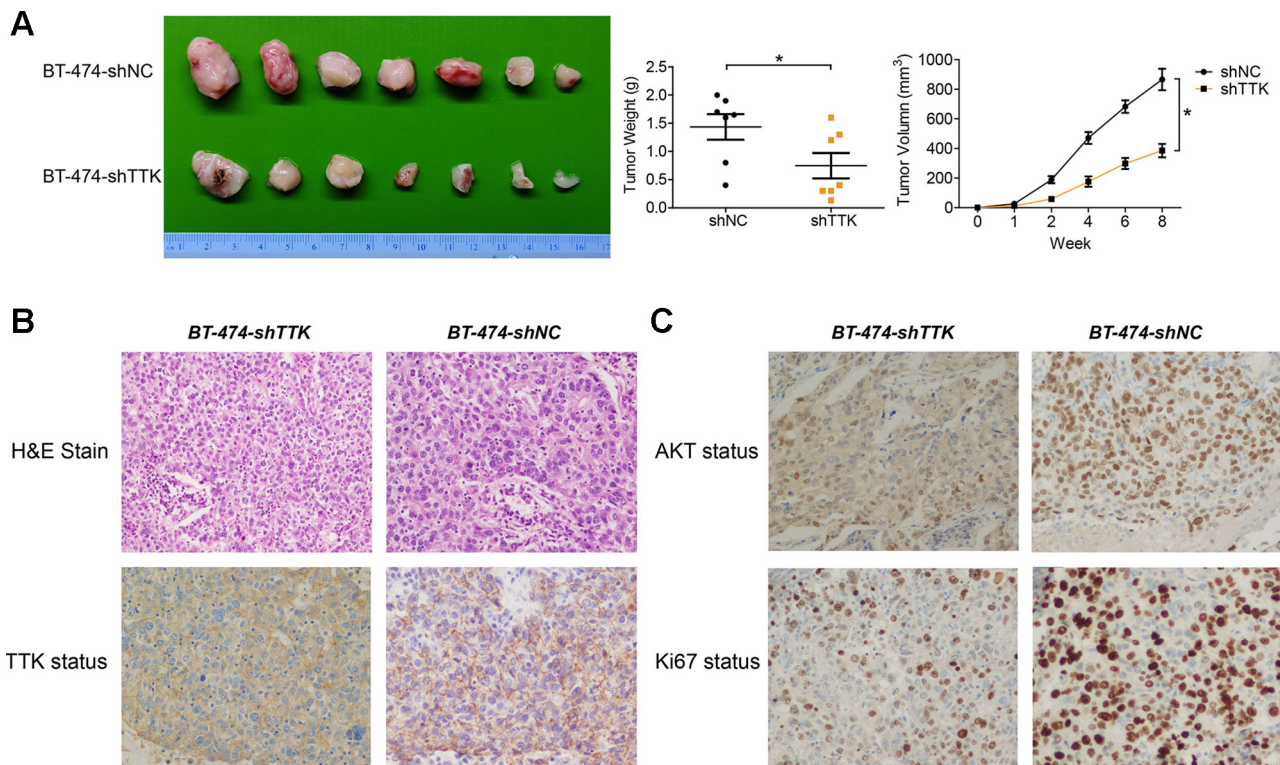


Figure 5. *TTK* knockdown inhibits the growth of triple positive breast cancer (TPBC) cells *in vivo*. **A**) Tumor xenograft weights and volumes of the *TTK*-knockdown and control groups. **B**) *TTK*, *AKT*, and *Ki-67* index expressions were lower in the *TTK*-knockdown and control groups than in the *TTK*-expressing group, as revealed by IHC of mouse tumor xenografts (original magnification, $\times 100$). Data are presented as the mean \pm SD. The data shown are representative results of three independent experiments. * $p < 0.05$

administered adjuvant trastuzumab as the anti-HER2 agent, along with chemotherapy and endocrine therapy.

Consistent with our results, AI-Ejeh et al. [17] revealed that TTK protein levels were elevated in aggressive tumors, leading to poor survival. Most previous TNBC studies focused on aberrant TTK expression in TNBCs, an event that is significantly associated with an elevated risk of relapse and docetaxel resistance [17, 18, 25, 26]. Based on these findings, we hypothesized that aberrant TTK expression facilitates the progression of TPBC. Accordingly, we found that TTK expression was significantly higher in TPBCs with a poor prognosis than in those with a good prognosis. Assessing TTK expression augments the prognostic information provided by the traditional prognostic indicators, namely ER, progesterone receptor, and HER2. This is the first study to evaluate the effect of TTK expression on the survival of a consecutive TPBC cohort.

To further investigate the functional role of TTK in the progression of TPBC, we used a lentivirus to achieve *TTK* knockdown in BT474 cells. *TTK* knockdown inhibited the proliferation, colony formation, and invasiveness of TPBC cells, both *in vivo* and *in vitro*. Additionally, *TTK* knockdown might affect the expression of proteins associated with proliferation and invasiveness. Recent research has indicated that TTK promotes cell migration and EMT by enhancing the expression of dihydropyrimidinase-like 3 (DPYSL3), thus promoting snail-regulated EMT, and reinforcing the metastatic potential and ultimately tumor metastasis in TPBC. *TTK* and *DPYSL3* upregulation was negatively correlated with clinical outcomes in patients with lung cancer [27]. Importantly, our findings revealed that TTK protein expression was positively correlated with tumor size, TNM stage, p53 mutation status, and the Ki-67 index. Consistent with our findings, previous studies have shown that TTK expression is significantly higher in breast cancers expressing a mutant p53 than in those expressing wild-type p53, independent of the breast cancer subtype [28]. In patients with breast cancer, TTK overexpression is associated with increased breast cancer grade and aggressiveness, possibly because it promotes the proliferation or survival of cancer cells [25].

The AKT signaling pathway can exert proliferative effects by targeting downstream transcription factors. TTK promotes cell proliferation and invasiveness by activating the AKT/mTOR and MDM2/p53 signaling pathways [29]. Our findings demonstrate that reducing TTK expression can inhibit the activation of AKT expression and proliferation in breast cancer cells. Many clinical trials [9–11, 13, 30–32] have assessed the effects of TTK inhibitors for TNBC treatment and shown that they might be effective as second-line therapy, and particularly for resistant patients; our findings are consistent with these results. Additional large cohort studies are required to validate the positive effects of anti-*TTK* therapy. In conclusion, TTK upregulation was closely associated with TPBC progression and poor prognosis. Thus, TTK

could serve as a valuable prognostic marker and therapeutic target for TPBC.

Acknowledgments: The authors would like to thank Dr. Yantong Guo for providing technical assistance.

References

- [1] BARROSO-SOUSA R, BARRY WT, GUO H, DILLON D, TAN YB et al. The immune profile of small HER2-positive breast cancers: a secondary analysis from the APT trial. *Ann Oncol* 2019; 30: 575–581. <https://doi.org/10.1093/annonc/mdz047>
- [2] LLOMBART-CUSSAC A, CORTES J, PARE L, GALVAN P, BERMEJO B et al. HER2-enriched subtype as a predictor of pathological complete response following trastuzumab and lapatinib without chemotherapy in early-stage HER2-positive breast cancer (PAMELA): an open-label, single-group, multicentre, phase 2 trial. *Lancet Oncol* 2017; 18: 545–554. [https://doi.org/10.1016/S1470-2045\(17\)30021-9](https://doi.org/10.1016/S1470-2045(17)30021-9)
- [3] GIORDANO SH, TEMIN S, KIRSHNER JJ, CHANDAR-LAPATY S, CREWS JR et al. Systemic therapy for patients with advanced human epidermal growth factor receptor 2-positive breast cancer: American Society of Clinical Oncology clinical practice guideline. *J Clin Oncol* 2014; 32: 2078–2099. <https://doi.org/10.1200/JCO.2013.54.0948>
- [4] CARDOSO F, COSTA A, SENKUS E, AAPRO M, ANDRE F et al. 3rd ESO-ESMO International Consensus Guidelines for Advanced Breast Cancer (ABC 3). *Ann Oncol* 2017; 28: 16–33. <https://doi.org/10.1093/annonc/mdw544>
- [5] VICI P, PIZZUTI L, NATOLI C, GAMUCCI T, DI LAURO L et al. Triple positive breast cancer: a distinct subtype? *Cancer Treat Rev* 2015; 41: 69–76. <https://doi.org/10.1016/j.ctrv.2014.12.005>
- [6] LARA-GONZALEZ P, WESTHORPE FG, TAYLOR SS. The spindle assembly checkpoint. *Curr Biol* 2012; 22: R966–980. <https://doi.org/10.1016/j.cub.2012.10.006>
- [7] LAUZE E, STOELCKER B, LUCA FC, WEISS E, SCHUTZ AR et al. Yeast spindle pole body duplication gene *MPS1* encodes an essential dual specificity protein kinase. *EMBO J* 1995; 14: 1655–1663.
- [8] XU Q, ZHU S, WANG W, ZHANG X, OLD W et al. Regulation of kinetochore recruitment of two essential mitotic spindle checkpoint proteins by *Mps1* phosphorylation. *Mol Biol Cell* 2009; 20: 10–20. <https://doi.org/10.1091/mbc.e08-03-0324>
- [9] HEWITT L, TIGHE A, SANTAGUIDA S, WHITE AM, JONES CD et al. Sustained *Mps1* activity is required in mitosis to recruit O-Mad2 to the Mad1-C-Mad2 core complex. *J Cell Biol* 2010; 190: 25–34. <https://doi.org/10.1083/jcb.2011002133>
- [10] JEMAA M, GALLUZZI L, KEPP O, SENOVILLA L, BRANDS M et al. Characterization of novel *MPS1* inhibitors with preclinical anticancer activity. *Cell Death Differ* 2013; 20: 1532–1545. <https://doi.org/10.1038/cdd.2013.105>

- [11] KWIATKOWSKI N, JELLUMA N, FILIPPAKOPOULOS P, SOUNDARARAJAN M, MANAK MS et al. Small-molecule kinase inhibitors provide insight into Mps1 cell cycle function. *Nat Chem Biol* 2010; 6: 359–368. <https://doi.org/10.1038/nchembio.345>
- [12] COLOMBO R, CALDARELLI M, MENNECOZZI M, GIORGINI ML, SOLA F et al. Targeting the mitotic checkpoint for cancer therapy with NMS-P715, an inhibitor of MPS1 kinase. *Cancer Res* 2010; 70: 10255–10264. <https://doi.org/10.1158/0008-5472.CAN-10-2101>
- [13] DANIEL J, COULTER J, WOO JH, WILSBACH K, GABRIELSON E. High levels of the Mps1 checkpoint protein are protective of aneuploidy in breast cancer cells. *Proc Natl Acad Sci USA* 2011; 108: 5384–5389. <https://doi.org/10.1073/pnas.1007645108>
- [14] YUAN B, XU Y, WOO JH, WANG Y, BAE YK et al. Increased expression of mitotic checkpoint genes in breast cancer cells with chromosomal instability. *Clin Cancer Res* 2006; 12: 405–410. <https://doi.org/10.1158/1078-0432.CCR-05-0903>
- [15] SALVATORE G, NAPPI TC, SALERNO P, JIANG Y, GARBI C et al. A cell proliferation and chromosomal instability signature in anaplastic thyroid carcinoma. *Cancer Res* 2007; 67: 10148–10158. <https://doi.org/10.1158/0008-5472.CAN-07-1887>
- [16] LING Y, ZHANG X, BAI Y, LI P, WEI C et al. Overexpression of Mps1 in colon cancer cells attenuates the spindle assembly checkpoint and increases aneuploidy. *Biochem Biophys Res Commun* 2014; 450: 1690–1695. <https://doi.org/10.1016/j.bbrc.2014.07.071>
- [17] AL-EJEH F, SIMPSON PT, SAUNUS JM, KLEIN K, KALIMUTHO M et al. Meta-analysis of the global gene expression profile of triple-negative breast cancer identifies genes for the prognostication and treatment of aggressive breast cancer. *Oncogenesis* 2014; 3: e100. <https://doi.org/10.1038/oncsis.2014.14>
- [18] MAIRE V, BALDEYRON C, RICHARDSON M, TESSON B, VINCENT-SALOMON A et al. TTK/hMPS1 is an attractive therapeutic target for triple-negative breast cancer. *PLoS One* 2013; 8: e63712. <https://doi.org/10.1371/journal.pone.0063712>
- [19] ELSTON CW, ELLIS IO. Pathological prognostic factors in breast cancer. I. The value of histological grade in breast cancer: experience from a large study with long-term follow-up. *Histopathology* 1991; 19: 403–410. <https://doi.org/10.1111/j.1365-2559.1991.tb00229.x>
- [20] WON KY, KIM GY, KIM YW, SONG JY, LIM SJ. Clinicopathologic correlation of beclin-1 and bcl-2 expression in human breast cancer. *Hum Pathol* 2010; 41: 107–112. <https://doi.org/10.1016/j.humpath.2009.07.006>
- [21] CAO L, SUN PL, YAO M, JIA M, GAO H. Expression of YES-associated protein (YAP) and its clinical significance in breast cancer tissues. *Hum Pathol* 2017; 68: 166–174. <https://doi.org/10.1016/j.humpath.2017.08.032>
- [22] LIVAK KJ, SCHMITTGEN TD. Analysis of relative gene expression data using real-time quantitative PCR and the 2⁻($\Delta\Delta C_T$) Method. *Methods* 2001; 25: 402–408. <https://doi.org/10.1006/meth.2001.1262>
- [23] NAITO S, VON ESCHENBACH AC, GIAVAZZI R, FIDLER IJ. Growth and metastasis of tumor cells isolated from a human renal cell carcinoma implanted into different organs of nude mice. *Cancer Res* 1986; 46: 4109–4115.
- [24] KAUFMAN B, MACKEY JR, CLEMENS MR, BAPSY PP, VAID A et al. Trastuzumab plus anastrozole versus anastrozole alone for the treatment of postmenopausal women with human epidermal growth factor receptor 2-positive, hormone receptor-positive metastatic breast cancer: results from the randomized phase III TAnDEM study. *J Clin Oncol* 2009; 27: 5529–5537. <https://doi.org/10.1200/JCO.2008.20.6847>
- [25] MAIA AR, DE MAN J, BOON U, JANSSEN A, SONG JY et al. Inhibition of the spindle assembly checkpoint kinase TTK enhances the efficacy of docetaxel in a triple-negative breast cancer model. *Ann Oncol* 2015; 26: 2180–2192. <https://doi.org/10.1093/annonc/mdv293>
- [26] GYORFFY B, BOTTAI G, LEHMANN-CHE J, KERI G, ORFIL L et al. TP53 mutation-correlated genes predict the risk of tumor relapse and identify MPS1 as a potential therapeutic kinase in TP53-mutated breast cancers. *Mol Oncol* 2014; 8: 508–519. <https://doi.org/10.1016/j.molonc.2013.12.018>
- [27] TSAI YM, WU KL, CHANG YY, HUNG JY, CHANG WA et al. Upregulation of Thr/Tyr kinase Increases the Cancer Progression by Neurotensin and Dihydropyrimidinase-Like 3 in Lung Cancer. *Int J Mol Sci* 2020; 21: 1640. <https://doi.org/10.3390/ijms21051640>
- [28] MORRISON CD, CHANG JC, KERI RA, SCHIEMANN WP. Mutant p53 dictates the oncogenic activity of c-Abl in triple-negative breast cancers. *Cell Death Dis* 2017; 8: e2899. <https://doi.org/10.1038/cddis.2017.294>
- [29] LIU X, LIAO W, YUAN Q, OU Y, HUANG J. TTK activates Akt and promotes proliferation and migration of hepatocellular carcinoma cells. *Oncotarget* 2015; 6: 34309–34320. <https://doi.org/10.18632/oncotarget.5295>
- [30] TARDIF KD, ROGERS A, CASSIANO J, ROTH BL, CIMBORA DM et al. Characterization of the cellular and antitumor effects of MPI-0479605, a small-molecule inhibitor of the mitotic kinase Mps1. *Mol Cancer Ther* 2011; 10: 2267–2275. <https://doi.org/10.1158/1535-7163.MCT-11-0453>
- [31] LIU Y, LANG Y, PATEL NK, NG G, LAUFER R et al. The Discovery of Orally Bioavailable Tyrosine Threonine Kinase (TTK) Inhibitors: 3-(4-(heterocycl)phenyl)-1H-indazole-5-carboxamides as Anticancer Agents. *J Med Chem* 2015; 58: 3366–3392. <https://doi.org/10.1021/jm501740a>
- [32] NAUD S, WESTWOOD IM, FAISAL A, SHELDRAKE P, BAVETSIAS V et al. Structure-based design of orally bioavailable 1H-pyrrolo[3,2-c]pyridine inhibitors of mitotic kinase monopolar spindle 1 (MPS1). *J Med Chem* 2013; 56: 10045–10065. <https://doi.org/10.1021/jm401395s>